IEEE Access
Multidisciplinary | Rapid Review | Open Access Journal

Received August 24, 2021, accepted October 17, 2021, date of publication November 11, 2021, date of current version December 3, 2021.

Digital Object Identifier 10.1109/ACCESS.2021.3127852

Towards an Increased Detection Sensitivity of Time-Delay Attacks on Precision Time Protocol

LEA SCHÖNBERGER[1], (Graduate Student Member, IEEE), MOHAMMAD HAMAD[2], JAVIER VELASQUEZ GOMEZ[3], SEBASTIAN STEINHORST[2], (Senior Member, IEEE), AND SELMA SAIDI[4], (Member, IEEE)

[1]Department of Computer Science, TU Dortmund University, 44221 Dortmund, Germany
[2]Faculty of Electrical Engineering and Information Technology, Technical University of Munich, 80333 Munich, Germany
[3]Institute of Embedded Systems, Hamburg University of Technology, 21073 Hamburg, Germany
[4]Department of Electrical Engineering and Information Technology, TU Dortmund University, 44221 Dortmund, Germany

Corresponding author: Lea Schönberger (lea.schoenberger@tu-dortmund.de)

This work was supported in part by the Deutsche Forschungsgemeinschaft (DFG) within the Collaborative Research Center SFB 876, project A2; in part by the Institute for Advanced Study, Technische Universität München, funded by the German Excellence Initiative and the European Union Seventh Framework Program under Grant 291763; and in part by the European Commission through the H2020 nIoVe: A Novel Adaptive Cybersecurity Framework for the Internet-of-Vehicle project under Grant 833742.

ABSTRACT Precision time protocol (PTP) is one of the most widely used protocols for clock synchronization in packet-switched networks, on which, among others, the transaction synchronization of the stock markets relies. PTP was not standardized with security as a core requirement and is therefore vulnerable and attractive to manifold kinds of malicious attacks, such as time-delay attacks (TDAs). TDAs, in short, corrupt the exchange of timestamped messages and thus cause an incorrect synchronization process. The annex P of the IEEE 1588-2019 standard has defined a number of security mechanisms for clock synchronization, but, however, none of these can protect a PTP-based system completely against TDAs. In this work, we enhance existing approaches by introducing a so-called observation task and analytically deriving attack parameters of an ongoing TDA. Following the recommendation of the annex P of the IEEE 1588-2019 standard, these attack parameters can serve as an additional input for intrusion detection systems and allow for a more reliable and sensitive detection of TDAs. In a comprehensive evaluation, we experimentally investigate the impact different attack parameter combinations can have on a system.

INDEX TERMS Precision time protocol, real-time, response time analysis, security, time-delay attack.

I. INTRODUCTION

Precision time protocol (PTP) is one of the most widely used protocols for clock synchronization in packet-switched networks and is based on the exchange of timestamped messages between clients and servers. Among others, it is adopted to synchronize transactions at the stock markets. In 2013, Eurex (one of the world's largest derivatives exchanges) was halted for a few hours due to an internal time synchronization issue,[1] which led to a major loss of profit for many investors. Although this incident was caused by an internal fault, its profound and harmful consequences point out the vulnerability of PTP, turning it into an attractive target for malicious attacks.

In fact, PTP was not standardized with security as a core requirement and therefore is vulnerable to manifold kinds of attacks. One of these is the so-called time-delay attack (TDA) [1]–[3], in the course of which – in short – an attacker, who gained access to the network, delays individual PTP-related messages, which leads to incorrect timestamps being used in the synchronization process. This can have various effects on the network and its participants, as we will discuss later on.

Although the annex P of the IEEE 1588-2019 standard [4] has defined a number of security mechanisms for clock synchronization, none of these measures can protect a PTP-based system completely against TDAs. For this reason, prong D of the annex P of the IEEE 1588-2019 standard does not only emphasize the importance of combining multiple security mechanisms, but specifically recommends to enhance the security of a PTP-based network by monitoring a broad range of parameters. Against this background, we complement

The associate editor coordinating the review of this manuscript and approving it for publication was Zhibo Wang.

[1]https://www.reuters.com/article/idINL6N0GR0TY20130826

existing approaches by making use of response time analysis techniques from the real-time domain and focusing on a parameter, which has, to the best of our knowledge, not yet been considered. By analytically deriving attack properties from the response time of a so-called observation task, we provide an additional input for intrusion detection systems, aiming to allow for a more reliable and sensitive detection of time-delay attacks.

In short, we make the following contributions:

- We introduce an observation task, which can be inserted into existing PTP-synchronized client systems and allows to indicate if a TDA is performed in the network, based on its response time.
- We analytically derive convergence properties of the busy window response time analysis method and exploit these to approximate the attack properties of an ongoing TDA, which can serve as an input to sophisticated intrusion detection systems and thus lead to an increased attack detection sensitivity.
- By means of comprehensive simulations, we explore the impact of the attack parameters of a TDA on the system.

The rest of this work is structured as follows: In Sec. II, we explain PTP in detail, before we introduce the threat model adopted in this work in Sec. III. In the course of this, we first clarify how time-delay attacks can be performed on PTP in Sec. III-A and, thereon, reveal our attacker model in Sec. III-B. In Sec. IV, we provide an overview about existing security and attack mitigation mechanisms with respect to PTP, motivating the novelty and necessity of our analysis proposed in Sec. V. We explore the impact of our derived attack parameters experimentally in Sec. VI, before we summarize our findings and conclude this work in Sec. VII.

II. PRECISION TIME PROTOCOL

PTP [4] is used for clock synchronization between different participants in a packet-switched network. In networks based on PTP, one participant's clock serves as the main clock (subsequently termed *server clock*) with respect to which all other participants' clocks need to be periodically adjusted. The synchronization process between the server and another network participant (henceforth termed *client*) is based on the exchange of timestamped messages, by means of which the clock offset, i.e., the difference between the server clock and the client clock, is computed. In the course of this, it is necessary to also determine the transmission delay, which is not part of the clock offset and therefore must be taken into consideration during the offset computation to ensure the correctness of the clock adjustment. In Fig. 1, a simplified network is portrayed, by means of which the synchronization process is explained in more detail: Initially, the server sends a *Sync* message to the client and timestamps the moment t_1, in which the message leaves the server. Depending on the implementation, this timestamp is transmitted to the client either via the *Sync* message or by using a so-called *Follow_Up* message. The client, in turn, timestamps the instant t_2 in which it receives the *Sync* message according to its local

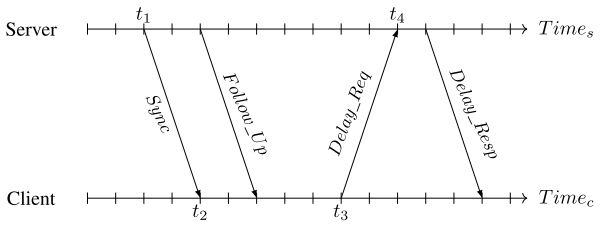

FIGURE 1. A simple network, in which PTP synchronization messages are exchanged. Based on [4].

clock. Thereon, it computes the difference between t_2 and t_1, which corresponds to the offset between its local clock and the server clock in addition to the transmission delay. To calculate the transmission delay, the client needs to measure the round-trip time to the server and back. For this purpose, it sends a *Delay_Req* message to the server and timestamps the moment t_3, in which the message leaves the client. Once a *Delay_Resp* message is received, which is sent by the server and contains the timestamp t_4 marking the arrival of the *Delay_Req* message at the server, the client extracts t_4 and proceeds with the computation.

Based on the four timestamps, i.e., t_1, t_2, t_3, and t_4, the client can estimate the transmission delay under the assumption that the transmission channel is symmetric,[2] i.e., that the time required for transmitting a message from the server to the client equals the time required for transmitting a message from the client to the server, as given by (1).

$$\text{transmission delay} = \frac{(t_2 - t_1) + (t_4 - t_3)}{2} \tag{1}$$

After having computed the transmission delay, the clock offset can be calculated as given by (2) and the client's clock can be updated accordingly.

$$\text{offset} = \frac{(t_2 - t_1) - (t_4 - t_3)}{2} \tag{2}$$

III. THREAT MODEL

In the following, we clarify the threat model considered in this work. First, we explain the principle of time-delay attacks on PTP in Sec. III-A, before we introduce the adopted attacker model in Sec. III-B.

A. TIME-DELAY ATTACKS ON PTP

As stated in Sec. II, the computation of the offset between a server clock and a client clock relies on the assumption that the communication channel is symmetric, which originates from the IEEE 1588-2019 standard [4] and constitutes a vulnerability attackers can exploit. By analyzing the network traffic, intercepting PTP messages, and artificially retaining (and thus delaying) *Sync* and/or *Delay_Req* messages, incorrect timestamps are retrieved by a client, which consequently computes a wrong clock offset and updates its clock incorrectly, as illustrated in Fig. 2a. For clarification, consider

[2]Note that this assumption is made according to the section 6.3.3 in the IEEE 1588-2019 standard [4].

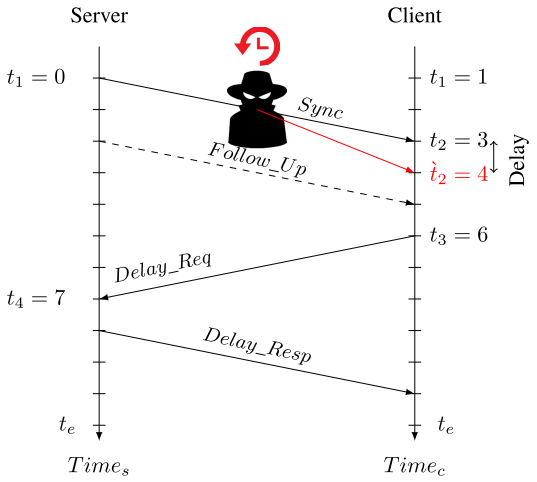

(a)

Item	No Attack	TDA
t_1	0	0
t_2	3	$\grave{t}_2 = 4$
t_3	6	6
t_4	7	7
offset	1	1.5
Clock_s at t_e	11	11
Clock_c at t_e	11	10.5

(b)

FIGURE 2. Timing effects of asymmetric delaying attacks on PTP messages: a) Representation of an exemplary attack. b) Effect on the offset calculation.

the offset computation process shown in Fig. 2. Initially, the client clock has an offset of +1 time units, which will be derived correctly if no TDA is performed. However, in the event of a TDA, the client will compute an incorrect offset of +0.5 time units. Please note that a late release instant of the *Delay_Req* message does not have an impact on the offset computation (which considers only t_4 and t_3), unless the *Delay_Req* message itself is affected by a time-delay attack.

A TDA can be performed in different ways, namely, it is possible to delay either all messages or to delay PTP messages only. Moreover, a TDA can be performed either in one direction of the communication, known as asymmetric link delay attack [5], or in both directions with different delays,[3] termed symmetric delay attack. However, for the remainder of this work, the TDA type is not relevant.

B. ATTACKER MODEL

For the rest of this work, we assume that the attacker is either an external entity or an insider with malicious intents [6]. We adopt an in-band adversary model [3], according to which the attacker has full control of the communication path between the server and its clients. However, since we assume the MACsec or IPsec protocol to be used for securing the communication between the server and its clients, inserting fake messages and changing fields of passing messages is detectable and therefore not an option. Instead, the attacker is supposed to aim at compromising the time synchronization of the system using time-delay attacks.

The server is assumed to be trustworthy, such that it cannot be compromised. Moreover, clients are assumed to be secure, so that the attacker cannot compromise them directly. Nevertheless, the attacker is expected to have the expertise and the tools to compromise a switch[4] and thus to be able to compromise all clients indirectly by performing time-delay attacks. Concretely, we assume that a man-in-the-middle attack is implemented in the course of which a TDA on PTP synchronization tasks is performed (as explained in [7]), which introduces asymmetric communication delays, leading to a change of the activation periods of message transmissions.

IV. RELATED WORK

Owing to the vulnerability of PTP with respect to security attacks, the challenge of securing PTP and providing detection as well as mitigation mechanisms has been extensively studied [3], [8].

First, the annex K of the IEEE 1588-2008 standard [9] introduced a number of mechanisms to improve the security of PTP. These were extended and enhanced in the latest, recently released version (i.e., in the annex P of IEEE 1588-2019 [4]) and include the deployment of security protocols such as MACsec [10] and IPsec [11] in order to ensure data origin authentication, communication confidentiality, data integrity, as well as replay attack protection and, in consequence, to prevent PTP message manipulation [8], message dropping and insertion [12], denial of service (DoS) attacks [13], as well as master node falsification attacks [14].

With respect to TDAs, multiple detection and mitigation strategies have been proposed in the literature, including architectural mechanisms such as the usage of multiple paths between the server and client clocks [1] or of multiple time sources, i.e., servers [4]. However, although such strategies are theoretically sound, they are not always practical due to their strong dependence on the network topology.

Another direction followed by the research community is to analyze the impact of TDAs on the calculation of the round-trip delay and offset at client nodes [2], [13] in order to develop better mitigation mechanisms. To detect a TDA, it is possible to use a predefined round-trip delay threshold [1], [15]: Whenever this threshold is exceeded, the client assumes that a TDA is in progress. Using this mechanism is, however, not always practical; for instance, if network delays are unbounded, false alarms may be triggered frequently [1]. Moreover, if an attacker permanently injects delays larger than the predefined threshold, a DoS attack may be introduced [2].

[3] An identical delay introduced into both directions does not have any effect on the behavior of the protocol.

[4] Explaining the initial exploit allowing the attacker to compromise the switch is beyond the scope of this work.

Apart from these works, much effort has been made to detect anomalies in general based on the timing behavior of a system. In [16], the worst-case execution time (WCET) of each code snippet of a task, as derived based on static timing analysis, is used to detect the execution of unauthorized code. More precisely, the system collects the task's timing metrics and compares them with predefined worst-case bounds. By doing this, the system becomes capable of detecting situations, in which the observed task is going to exceed its timing requirements due to a security breach. Instead of monitoring at the software level, the usage of dedicated hardware for monitoring the execution of code snippets is proposed in [17]. The monitored timing values are compared with precomputed WCET bounds, which allows to detect deviations. Applying worst-case response time analysis for deriving a new bound on the response time of a task and using this as an indicator of code injection attacks has been suggested in [18].

To the best of our knowledge, response-time analysis-based techniques have not yet been applied with regard to the detection of TDAs on PTP. Against this background, we follow the recommendation of the prong D of the annex P of the IEEE 1588-2019 standard [4], according to which the security of a PTP-based network should be enhanced by, in addition to other measures, monitoring a broad range of parameters in the network. Specifically, we subsequently derive attack properties from the response time of an observation task, which can serve as an additional input for intrusion detection systems.

V. TIMING ANALYSIS

As discussed in Sec. IV, it is meaningful to monitor a large number of parameters in order to detect time-delay attacks and to be able to invoke countermeasures. Although the number of parameters that can be monitored is large, not all of them are useful in this context. For instance, when considering a client system on which one or more tasks are delayed due to a TDA in the network (cf. Sec. III), monitoring the execution time of tasks is not meaningful for detecting the attack. In fact, the events of the respective tasks are delayed, but none is skipped, for which reason the TDA does not have any impact on their execution times.[5] What, in contrast, is affected during a TDA is the response time of tasks, as illustrated in the example in Fig. 3: If the activation of the higher-priority task τ_j is delayed by δ time units (cf. second diagram in Fig. 3), the response time of the lower-priority task τ_k is shorter compared to the case in which the activation of τ_j is not delayed (cf. first diagram in Fig. 3). Accordingly, observing the response time of tasks on a client system appears to be a promising approach in order to detect TDAs in the network.

However, monitoring the response times of all (PTP-synchronized) tasks on all client systems in a network is inconvenient. For this reason, we subsequently introduce so-called *observation tasks*, which are scheduled under the lowest priority on each client system (strategies for integrating an observation task into an existing system can, e.g., be found in [19]). The response time of an observation task includes the interference from all higher-priority tasks and therefore reflects the effects of delays following from a TDA. Instead of simply comparing the observed response time of an observation task with the so-called *nominal worst-case response time*, i.e., the worst-case response time in the case that no TDA is performed in the network, we go one step further in this work and derive attack parameters from the observed response time, which can be used by intrusion detection systems to not only detect a TDA, but also to invoke countermeasures.

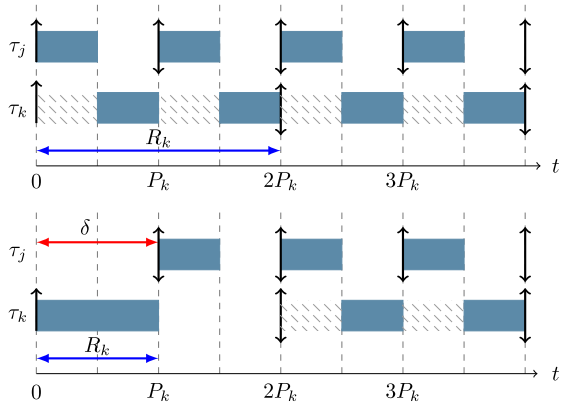

FIGURE 3. An example illustrating the effect of a delayed activation of the higher-priority task τ_j on the response time of the lower-priority task τ_k (second diagram) in comparison to a case in which the activation of τ_j is not delayed (first diagram).

To this end, we subsequently provide a system model in Sec. V-A and model the timing behavior of the system in Sec. V-B, before we revisit the theoretical foundations of the busy window response time analysis in Sec. V-C and derive convergence properties, which are exploited in Sec. V-D to obtain approximations of the attack parameters of a TDA. In Sec. V-E, we provide some additional remarks. A supportive quick reference for the notation is given in Table 1.

A. SYSTEM MODEL

For the rest of this work, we consider a client system in a PTP-based network, on which a set of tasks T is assumed to be executed under a preemptive fixed-priority scheduling policy according to a given priority assignment. Each task $\tau_i \in T$ is characterized by its *worst-case execution time (WCET)* C_i and its *period* (or *minimum inter-arrival time*)[6] P_i. Moreover, α_i describes the *nominal event arrival function* of a task τ_i

[5]Note that monitoring the execution times of tasks may be meaningful to detect other attacks such as code injection attacks, where additional instructions are inserted by an attacker. However, this is beyond the scope of this work.

[6]Note that we focus on a set of sporadic tasks, which are activated by incoming messages. The time between the activation of two task instances is assumed to be at least the minimum inter-arrival time. If tasks are activated exactly according to the minimum inter-arrival time, the task behavior becomes periodic. Additionally, periodic tasks without message-based activation may be executed on the client system.

TABLE 1. An overview of the notation used in this work.

Notation	Explanation
α_i	nominal event arrival function (upper bound) of task τ_i
$\tilde{\alpha}_i$	off-nominal event arrival function (upper bound) of task τ_i
C_i	worst-case execution time (WCET) of task τ_i
d_i	number of delayed events of task τ_i due to a TDA
δ	fixed periodic delay resulting from a TDA
δ^{min}	minimum possible periodic delay attack
δ^{max}	maximum possible periodic delay without causing a DoS
f_i	computation function of the busy window of task τ_i
$f_i(n)$	computation function of the busy window of task τ_i at iteration n
$F_i(n)$	bound on the computation function of the busy window of task τ_i
$\phi_i(q)$	q-event earliest possible activation of task τ_i
I_i	set of interferers of task τ_i, i.e., tasks with higher priority
I_i^{non}	set of interferers of task τ_i, which are not affected by a TDA
I_i^{tda}	set of interferers of task τ_i, which are affected by a TDA
ℓ_i	number of periodic events of task τ_i after which one event is delayed
ℓ_i^{min}	minimum possible value of ℓ_i for task τ_i
ℓ_i^{max}	maximum possible value of ℓ_i for task τ_i
n_{tda}	convergence iteration of the computation function of the busy window of a task
P_i	period of a task τ_i
R_i	worst-case response time (WCRT) of task τ_i
ρ_i	rate of convergence of the computation function of the busy window of task τ_i
T	set of tasks on the contemplated client
τ_i	task; general notion
τ_j	interfering task of τ_k
τ_k	observation task with lowest priority
$w_i(q)$	q-event busy window of task τ_i
w_i	1-event busy window of task τ_i
w_i^n	size of the 1-event busy window of task τ_i at iteration n
Ω	overall delay introduced to the client system due to a TDA

providing an upper bound on the number of resource accesses per period of time. For each task τ_i, the set of *interferers*, i.e., the set of higher-priority tasks, is denoted as I_i. The activation of (a subset of) tasks is synchronized using PTP synchronization operations (cf. Sec. II).

In the following, the asymmetric communication delay resulting from the TDA (cf. Sec. III) as perceived from the perspective of the client system is modeled as a fixed periodic delay δ, which is introduced at particular activation periods during the so-called *attack window*, i.e., from the beginning until the end of an attack. Since delaying PTP synchronization messages for a longer time can result in an easily detectable denial of service (DoS) attack on the client node, we assume the fixed periodic delay δ to be at most δ^{max}. Note that δ^{max} depends on the network design and the configurations of the employed intrusion detection system, but is not an intentionally chosen design parameter. We assume that δ^{max} can be observed by an attacker as described in Sec. III-B, who is able to intercept and thus to analyze the network traffic.

B. TIMING AND EVENT MODEL

In order to analyze the response time of an observation task τ_k, it is necessary to first define the previously mentioned nominal worst-case response time of a task as well as the method by means of which it is computed. Concretely, the observation task is analyzed during a *busy window* $w_k(q)$, which is defined as follows:

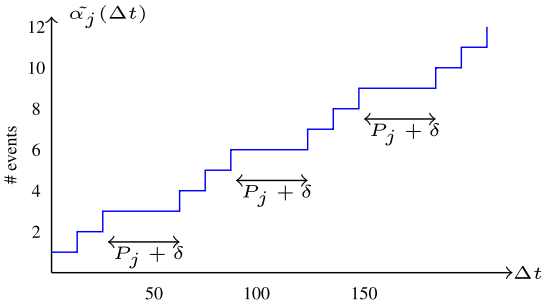

FIGURE 4. Off-nominal event arrival function of a task τ_j, where due to a TDA a delay of δ time units is inserted after every $\ell_j = 3$ events.

Definition 1 (Busy Window): Let the busy window $w_k(q)$ *be the maximum amount of time required to complete q activations of task τ_k. It is bounded by*

$$w_k(q) \leq q \cdot C_k + \sum_{\tau_j \in I_k} \alpha_j(w_k(q)) \cdot C_j. \tag{3}$$

Based on Def. 1, the *nominal worst-case response time* R_k of task τ_k is defined as follows:

Definition 2 (Nominal Worst-Case Response Time): The nominal worst-case response time R_k of a task τ_k is defined as

$$R_k = \max_{q \geq 1} \{w_k(q) - \phi_k(q) \mid \phi_k(q+1) \leq w_k(q)\}, \tag{4}$$

i.e., as the longest time interval between the activation and the completion of τ_k, which equals the difference between the busy window $w_k(q)$ and the earliest possible activation $\phi_k(q)$.

It is evident from Def. 1 that $w_k(q)$ of the analyzed task τ_k strongly depends on the nominal event arrival functions α_j of its interferers $\tau_j \in I_k$. However, in the case that a TDA is performed in the network, a delay is introduced to a number of tasks in I_k, as described above, which leads to a deviation from their nominal event arrival functions. To model the effect of a TDA on a task $\tau_j \in I_k$, an *off-nominal event arrival function* $\tilde{\alpha}_j$ over an interval of time Δt can be defined, for which holds that

$$\tilde{\alpha}_j(\Delta t) \leq \alpha_j(\Delta t) \; \forall \Delta t. \tag{5}$$

According to the threat model provided in Sec. III, we subsequently assume that due to the delayed activation of a task τ_j every $(\ell_j + 1)^{th}$ event within the attack window is delayed by δ time units, as illustrated in Fig. 4. With respect to all non-delayed events, i.e., where $\mod(\ell_j + 1) \neq 0$, the minimum distance between two subsequent events remains unchanged and thus equals the task period P_j. Accordingly, the off-nominal event arrival function $\tilde{\alpha}_j$ of a delayed task τ_j can be defined as follows:

Definition 3 (Off-Nominal Event Arrival Function): The off-nominal event arrival function of a task τ_j is defined as the sporadically periodic event function

$$\tilde{\alpha}_j(\Delta t) = \left\lfloor \frac{\Delta t}{\ell_j P_j + \delta} \right\rfloor \ell_j + \left\lceil \frac{\Delta t - \left\lfloor \frac{\Delta t}{\ell_j P_j + \delta} \right\rfloor (\ell_j P_j + \delta)}{P_j} \right\rceil. \tag{6}$$

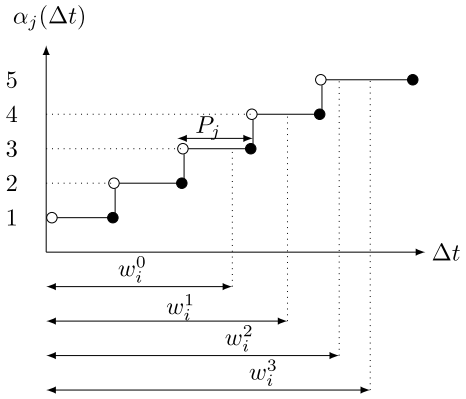

(a) Activations of interfering tasks.

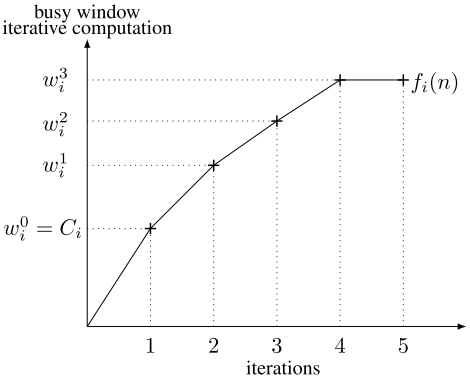

(b) The number of analysis iterations.

FIGURE 5. **Busy window computation dynamics of a task τ_i.**

For clarification, consider each complete sequence of ℓ_j events followed by a time interval of $P_j + \delta$ as a *section* of the interval Δt: The first part of Eq. 6 counts the number of events in all complete sections in Δt, while the second part of Eq. 6 factors in the remaining events. Note that the number of events within Δt computed by $\tilde{\alpha}_j$ is an upper bound.

Being able to quantify the events of a delayed task using the off-nominal event arrival function given in Def. 3, it is necessary to redefine the busy window introduced in Def. 1 in order to include the impact of the off-nominal interference of one or more[7] delayed $\tau_j \in I_k$ on the response time of the observation task τ_k:

Definition 4 (Busy Window Revisited): Let the busy window $w_k(q)$ be the maximum time required to complete q activations of task τ_k. It is bounded by

$$w_k(q) \leq q \cdot C_k + \sum_{\tau_j \in I_k^{tda}} \tilde{\alpha}_j(w_k(q)) \cdot C_j + \sum_{\tau_j \in I_k^{non}} \alpha_j(w_k(q)) \cdot C_j \tag{7}$$

where I_k^{tda} is the set of interferers of τ_k delayed due a TDA in the network and I_k^{non} is the set of non-delayed interferers, for which holds that $I_k^{tda} \cup I_k^{non} = I_k$ and $I_k^{tda} \cap I_k^{non} = \emptyset$.

Note that Def. 4 boils down to Def. 1 if no TDA is performed in the network, i.e., if $I_k^{tda} = \emptyset$.

So far, the nominal event arrival function of tasks as well as the nominal worst-case response time of the observation task τ_k have been defined, allowing us to compare the latter to the actual response time of τ_k in order to identify deviations. However, we are interested in retrieving more information about a TDA based on such deviations, namely, the so-called attack parameters, i.e., approximations of the delay δ, the overall delay Ω introduced to the client system, and the number of events ℓ_j after which one event of a task τ_j is delayed. Since the off-nominal event arrival functions $\tilde{\alpha}_j$ of delayed tasks $\tau_j \in I_k$, which depend on δ and ℓ_j (cf. Def. 3), are unknown, it is necessary to bridge the gap between these and the actual response time of the observation task τ_k. In the following, we dive deeper into the theory of the busy-window method and derive convergence properties, that can be exploited for this purpose.

[7]Remember that the switch's clock, but not the client's clock is corrupted. Therefore, on the client, only tasks activated by PTP synchronization tasks sent by the switch are delayed.

C. CONVERGENCE PROPERTIES OF THE BUSY-WINDOW METHOD

As evident from Def. 4, the busy window is calculated by a fixed-point computation, which is solved iteratively in a number of discrete steps. To facilitate the readability, we subsequently consider the computation of a one-event busy window, i.e., $q = 1$, for a task τ_i. In this contemplated case, the computation starts at iteration 0, where $w_i^0 = C_i$, i.e., considering only the WCET of τ_i without any interference. Thereon, one of the interferers I_i is added in each iteration, until the computation reaches a fixed point. This process is illustrated on the left side of Fig. 5.

Let $f_i(n) = w_i^n$ be a discrete function associating to each iteration n a value w_i^n describing the size of the busy window. This function f_i is referred to as the *computation function* of the busy window and is illustrated on the right side of Fig. 5. Although the computation function f_i is not known a priori, a bound can be obtained using numerical analysis. To this end, we make the following assumptions:

(a) The event arrival functions of all $\tau_i \in T$ are sub-additive, preventing the size of the busy window from growing asymptotically.

(b) When the workload of no not already considered $\tau_j \in I_i$ can be added from one iteration to the next one, the busy window converges and its size reaches a fixed point of value w_i^n. That is,

$$w_i^{n+1} - w_i^n = 0 \Leftrightarrow \sum_{j \in I_i} \alpha_j(w_i^n) - \sum_{j \in I_i} \alpha_j(w_i^{n-1}) = 0 \tag{8}$$

Aiming to bound the computation function f_i of the busy window of a task τ_i, it is necessary to reflect upon its *rate of convergence*. In general, the rate of convergence $\frac{f_i(n+1)-r}{f_i(n)-r}$

determines the ratio between the error[8] at iteration $n+1$ and the error at the previous iteration. Since r is not known in advance, the error $f_i(n)-r$ at iteration n is approximated with the value $f_i(n)-f_i(n-1)$.

For the specific $f_i(n) = w_i^n$ considered in this work, the following lemma can be formulated:

Lemma 1 (Rate of Convergence): For the rate of convergence ρ_i of the computation function f_i of the busy window of a task τ_i, it holds that

$$\rho_i = \frac{w_i^{n+1} - w_i^n}{w_i^n - w_i^{n-1}} \leq \sum_{\tau_j \in I_i} \frac{C_j}{P_j} \leq 1. \tag{9}$$

Proof: In order to determine the rate of convergence ρ_i, it is necessary to consider the difference of the size of the busy window between two iterations w_i^{n+1} and w_i^n. According to Def. 1, for a 1-event busy window, $w_i^{n+1} = C_i + \sum_{\tau_j \in I_i} \alpha_j(w_i^n) \cdot C_j$ and $w_i^n = C_i + \sum_{\tau_j \in I_i} \alpha_j(w_i^{n-1}) \cdot C_j$. Therefore, $w_i^{n+1} - w_i^n = \sum_{\tau_j \in I_i} \alpha_j(w_i^n) \cdot C_j - \sum_{\tau_j \in I_i} \alpha_j(w_i^{n-1}) \cdot C_j = \sum_{\tau_j \in I_i} \left\lceil \frac{w_i^n}{P_j} \right\rceil \cdot C_j - \sum_{\tau_j \in I_i} \left\lceil \frac{w_i^{n-1}}{P_j} \right\rceil \cdot C_j \leq \sum_{\tau_j \in I_i} \left(\frac{w_i^n}{P_j} + 1 \right) \cdot C_j - \sum_{\tau_j \in I_i} \left(\frac{w_i^{n-1}}{P_j} + 1 \right) \cdot C_j = \sum_{\tau_j \in I_i} \frac{w_i^n \cdot C_j}{P_j} + \sum_{\tau_j \in I_i} C_j - \sum_{\tau_j \in I_i} \frac{w_i^{n-1} \cdot C_j}{P_j} - \sum_{\tau_j \in I_i} C_j$. Thus, $w_i^{n+1} - w_i^n \leq \left(w_i^n - w_i^{n-1} \right) \cdot \sum_{\tau_j \in I_i} \frac{C_j}{P_j} \Leftrightarrow \frac{w_i^{n+1} - w_i^n}{w_i^n - w_i^{n-1}} \leq \sum_{\tau_j \in I_i} \frac{C_j}{P_j}$. Following from the schedulability condition for fixed-priority preemptive scheduling given in [20], $\sum_{\tau_j \in I_i} \frac{C_j}{P_j} \leq 1$. □

Based on the rate of convergence of the computation function f_i of the busy window, it is possible to determine a bound on f_i:

Theorem 1 (Bound on the Computation Function): The computation function $f_i(n)$ of the busy window of a task τ_i is bounded by the function

$$F_i(n) = \rho_i^n \cdot (w_i^1 - w_i^0). \tag{10}$$

Proof: The difference between two computation iterations of the busy window is defined as $F_i(n) = w_i^{n+1} - w_i^n$ at iteration n. It can also be defined based on the value of the busy window at the previous iteration $n-1$, taking into account the rate of convergence, which determines the error between the two iterations, i.e., $F_i(n) = \rho_i \cdot (w_i^n - w_i^{n-1})$. This can be further repeated until the initial iteration, taking into account the error by considering the rate of convergence ρ_i at each iteration. □

In what follows, we exploit the above derived convergence properties of the busy window method to retrieve approximations of the attack parameters of a TDA based on the response time of an observation task τ_k.

D. APPROXIMATION OF THE ATTACK PARAMETERS

As explained in Sec. V-B, the response time of an observation task τ_k does not equal its nominal worst-case response time if a TDA is performed in the network, but the size of the busy window is reduced due to the delayed events of a (number of) higher-priority task(s) $\tau_j \in I_k$, as stated in Def. 4. We refer to this reduced busy window by w_k^{tda} and assume that $w_k^{tda} < w_k$, where w_k corresponds to the nominal WCRT of τ_k. Moreover, we assume that the computation function f_k of the busy window converges at iteration n_{tda} – which is unknown, but can be derived as follows:

Theorem 2 (Convergence Iteration): The iteration n_{tda} at which the computation function f_k of the busy interval of a task τ_k converges and the size of the busy window reaches w_k^{tda} is given by

$$n_{tda} = \begin{cases} log_{\rho_k} \left(1 - \frac{(w_k^{tda} - C_k)(1-\rho_k)}{w_k^1 - w_k^0} \right) - 1 & \text{if } \rho_k < 1 \\ \frac{w_k^{tda} - C_k}{w_k^1 - w_k^0} - 1 & \text{if } \rho_k = 1 \end{cases} \tag{11}$$

where w_k^{tda} indicates the observed response time of τ_k. Proof: The value w_k^{tda} can be written as $w_k^{tda} = C_k + \sum_{n=0}^{n_{tda}} F_k(n)$, which equals the value of w_k^0 at the first iteration plus the accumulated difference of the added interference between two successive iterations until iteration n_{tda}. Using Theorem 1, $w_k^{tda} = C_k + \sum_{n=0}^{n_{tda}} \rho_k^n \cdot (w_k^1 - w_k^0) = C_k + (w_k^1 - w_k^0) \cdot \sum_{n=0}^{n_{tda}} \rho_k^n$. The term $\sum_{n=0}^{n_{tda}} \rho_k^n$ is a geometric series, for which two cases must be distinguished, namely, case i) $\rho_k < 1$ and case ii) $\rho_k = 1$. We first consider case i), in which, due to the nature of the geometric series, $\sum_{n=0}^{n_{tda}} \rho_k^n = \rho_k^0 \cdot \frac{1-\rho_k^{n_{tda}+1}}{1-\rho_k}$. By inserting and rearranging, $\rho_k^{n_{tda}+1} = 1 - \frac{\left(w_k^{n_{tda}} - C_k\right) \cdot (1-\rho_k)}{w_k^1 - w_k^0} \Leftrightarrow n_{tda} = \log_{\rho_k} \left(1 - \frac{\left(w_k^{n_{tda}} - C_k\right) \cdot (1-\rho_k)}{w_k^1 - w_k^0} \right) - 1$. In case ii), due to the nature of the geometric series, $\sum_{n=0}^{n_{tda}} \rho_k^n = \rho_k^0 \cdot \left(n^{tda} + 1 \right)$. Therefore, $w_k^{tda} = C_k + \left(w_k^1 - w_k^0 \right) \cdot \left(n^{tda} + 1 \right) \Leftrightarrow n^{tda} = \frac{w_k^{tda} - C_k}{w_k^1 - w_k^0} - 1$. □

Knowing the iteration n_{tda} at which the computation function f_k of the busy interval of the observation task τ_k converges, it is possible to approximate a number of attack parameters of an ongoing TDA. For this purpose, we subsequently first assume that only one $\tau_j \in I_k$ is delayed in consequence of a TDA. In this case, the overall delay Ω introduced to the client system as well as the number of delayed events $\tilde{q}_j$ per delayed task τ_j can be computed as follows:

Theorem 3 (Overall Delay and Delayed Events): The overall delay Ω introduced to the client system due to a TDA delaying one interferer $\tau_j \in I_k$ is given by

$$\Omega = f_k(n_{tda} + 1) - f_k(n_{tda}) \tag{12}$$

[8] An error at an iteration n refers the difference between the value $f_i(n)$, i.e., at iteration n, and the value of the fixed point r.

and the number of delayed events $\tilde{q}_j$ of τ_j by

$$\tilde{q}_j = \left\lceil \frac{\Omega}{P_j} \right\rceil. \tag{13}$$

Proof: Since we already discussed the properties of the convergence function f_k of the busy interval in Sec. V-C, we only sketch the proof. As illustrated in Fig. 6, it holds by construction that $f_k(n_{tda}+1) = f_k(n_{tda}) + \Omega$. Following from the assumption that only one $\tau_j \in I_k$ is delayed in consequence of a TDA, only events of τ_j can have been delayed during Ω. Therefore, the number of delayed events of τ_j is upper-bounded by $\tilde{q}_j = \left\lceil \frac{\Omega}{P_j} \right\rceil$. □

Having considered the case that only one $\tau_j \in I_k$ is delayed in consequence of a TDA, we henceforth assume that multiple $\tau_j \in I_k$ are delayed. While this assumption does not have any impact on the overall delay Ω, no definite statement about the number of delayed events per task can be made in this case. Since it is unknown, which task contributed how much to Ω, and since finding a distribution of Ω that corresponds to the real system state is not trivial, we suggest to approximate it by means of a heuristic.

As a straightforward approach to approximate the number of delayed events per task under the assumption that the number of delayed tasks is known, it is possible to distribute Ω according to a uniform distribution. However, since not all tasks contribute the same amount of workload to the busy window w_k^{tda}, it is more sensible to distribute Ω proportionally to the task utilization. For clarification, consider two tasks $\tau_j, \tau_y \in I_k$ delayed in consequence of a TDA, to which, proportionally to their utilization, i.e., $\frac{C_j}{P_j}$ and $\frac{C_y}{P_y}$, respectively, the following shares of Ω are distributed: $s_j \cdot \Omega$ to τ_j and $s_y \cdot \Omega$ to τ_y, where $s_j + s_y = 1$. Based on this distribution, the number of delayed events per task can be approximated similarly to Theorem 3, i.e., $\tilde{q}_j = \left\lceil \frac{s_j \cdot \Omega}{P_j} \right\rceil$ and $d_y = \left\lceil \frac{s_y \cdot \Omega}{P_y} \right\rceil$. If the number of delayed tasks, however, is unknown, all possible combinations of potentially delayed tasks must be enumerated and the approximated number of delayed events for each enumerated scenario must be computed in order to cover all possible system states.

Although the number of delayed events per task can be determined (in case only one task is delayed) or at least approximated and enumerated (in case multiple tasks are delayed), determining the exact periodic delay δ is not possible, since not only δ, but also ℓ_j and, in consequence, $\tilde{\alpha}_j$ are unknown. Nevertheless, bounds on δ can be provided: As already known from Sec. V-A, δ is upper-bounded by δ^{max}. To determine a lower bound δ^{min}, we again first consider the case that only one $\tau_j \in I_k$ is affected by a TDA. Since in this case the number of delayed events can be computed using Theorem 3, δ^{min} is obtained by:

Theorem 4 (Minimum Periodic Delay): The minimum periodic delay δ^{min} that can have been introduced to a PTP-synchronized interferer $\tau_j \in I_k$ of the observation task τ_k due to a TDA is given by

$$\delta^{min} = \frac{\Omega}{\alpha_j(w_k) - \tilde{q}_j} \tag{14}$$

Proof: Since the number of events of task τ_j during the nominal busy window w_k of the observation task τ_k can be determined by its well-known nominal event arrival function $\alpha_j(w_k)$, the number of events of task τ_j during the off-nominal busy window w_k^{tda} of τ_k can be computed as $\alpha_j(w_k) - \tilde{q}_j$, where $\tilde{q}_j$ is the number of delayed events. Although the number ℓ_i of periodic activations of τ_j after which one event is delayed by δ time units is unknown, the minimum possible value of ℓ_j according to the threat and system models is $\ell_j^{min} = 1$, which corresponds to the case that each event is delayed. Therefore, δ^{min} is obtained by dividing the overall introduced delay Ω by the number of events, i.e., $\delta^{min} = \frac{\Omega}{\alpha_j(w_k) - \tilde{q}_j}$. □

The approximation of δ^{min} and the knowledge of δ^{max} do not allow to determine the exact delay δ, but can be used to enumerate all possible values of δ. This enumeration can, for instance, be done by starting from $\ell_j = \ell_j^{min} = 1$ and increasing the value of ℓ_j in discrete steps, where the related value of δ can be computed similarly to Theorem 4, dividing Ω by the number of ℓ_j-event sections. All possible values of δ have been enumerated as soon as one computed value of δ is larger than δ^{max}. Then, $\ell_j^{max} = \ell_j - 1$, where ℓ is the value used in the recently completed computation. In the case that more than one $\tau_j \in I_k$ is delayed in consequence of a TDA, the same approach can be applied, however, taking all approximations of $\tilde{q}_j$ for all delayed $\tau_j \in I_k$ into account.

E. REMARKS ON THE ANALYSIS

So far, we derived convergence properties from the busy window response time analysis method and used these to retrieve attack parameters of an ongoing TDA. In this context, we append two further remarks:

1) The derived attack parameters are approximations and are not required to be precise. This is particularly the case because they are intended to be fed into an intrusion detection system *in addition* to many further parameters and, therefore, play a supportive role. More specifically, the intrusion detection system does not rely on the attack parameters, but can exploit these in order to make more sensitive predictions and to invoke more effective countermeasures.
2) It is well-known that in the majority of cases tasks do not execute for their worst-case execution time. However, in our formal analysis, we consider their worst-case execution times anyway. This follows from the fact that the applied busy window response time analysis technique is designed for analyzing the *worst-case* response time of tasks and therefore relies on the usage of worst-case execution time values. This may introduce a high degree of pessimism into our approach and could lead to an overly sensitive intrusion detection system triggering frequent false alarms, but can be avoided if realistic *worst average-case* execution time values are provided.

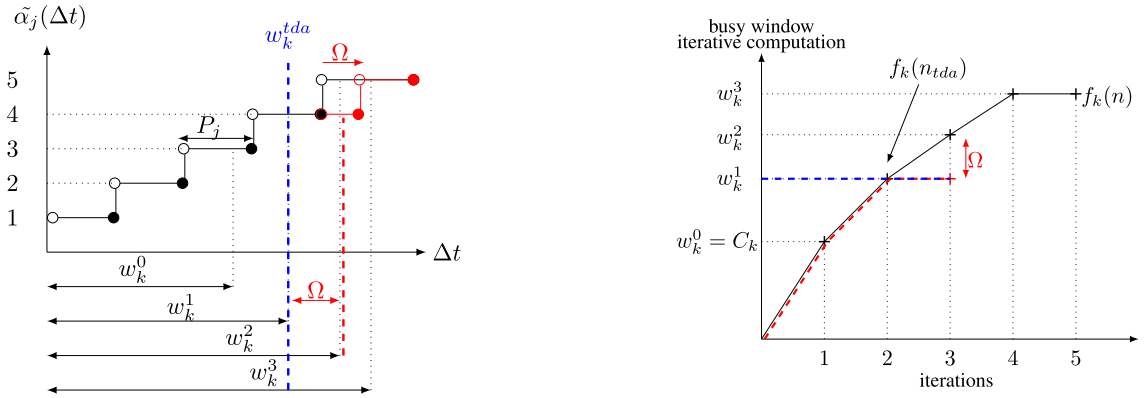

(a) Activations of interfering tasks.

(b) The number of analysis iterations.

FIGURE 6. Busy window computation dynamics of the observation task τ_k under the overall introduced delay Ω, simplified as an accumulation of all occurrences of δ.

It can also be meaningful to apply other execution time analyses such as the typical worst-case execution time analysis [18].

F. REMARKS ON JITTERS

In the following, we will discuss the impact of jitters on the analysis proposed in this work. Jitters are deviations of the event arrival from a task's period. More precisely, an event can arrive earlier (negative jitter) or later (positive jitter) than the period due to environmental influences such as, e.g., the material characteristics of a hardware component. A jitter is extremely small compared to a task period and can be bounded by the maximum negative jitter J_i^- and the maximum positive jitter J_i^+ for a task τ_i. Typically, a jitter is in the interval $\left[J_i^-, J_i^+\right]$ and occurs at every event release. However, the maximum jitters occur only in very rare cases.

Based on the maximum jitters, an upper and a lower bound on the nominal event arrival function α_i can be defined, namely, the nominal event arrival function with maximum negative jitter α_i^- and the nominal event arrival function with maximum negative jitter α_i^+, where the maximum negative (or positive, respectively) jitter occurs in each period.

Definition 5 (Nominal Event Arrival Functions with Maximum Jitter): The nominal event arrival function with maximum negative jitter of a task τ_i is defined as

$$\alpha_i^-(\Delta t) = \left\lceil \frac{\Delta t}{P_i - J_i^-} \right\rceil \tag{15}$$

and the nominal event arrival function with maximum positive jitter of a task τ_i is defined as

$$\alpha_i^+(\Delta t) = \left\lceil \frac{\Delta t}{P_i + J_i^+} \right\rceil. \tag{16}$$

Similarly, an off-nominal event arrival function with maximum negative jitter $\tilde{\alpha}_i^-$ and with maximum positive jitter $\tilde{\alpha}_i^+$ can be defined.[9]

[9]We omit the definitions at this point.

Consider the case that under a no-attack scenario each event of a task τ_j arrives with the maximum positive jitter J_j^+, as illustrated on the left side of Fig. 7. In consequence, the accumulation of jitters may at some point in time[10] equal the length of one period, such that until this point in time one event less has arrived compared to the zero-jitter case. Accordingly, the accumulated jitter will have an impact on the response time of the observation task and, therefore, is likely to be considered as a delay introduced by a TDA. However, such a scenario can only occur if the jitter is large enough compared to the period and, moreover, if the observation interval is long enough.

Further, consider the case that a TDA is performed, resulting in an off-nominal event arrival function $\tilde{\alpha}_j$ of task τ_j including a constant delay δ, as illustrated on the right side of Fig. 7. Additionally, assume that each event of τ_j arrives with a maximum negative delay J_j^-. In this scenario, the accumulated J_j^- may have amortized the delay δ at some point in time, such that the attack does not have any impact on the response time of the observation task. However, similar to the previous case, this can only occur if the jitter is large enough compared to the period, if the observation interval is long enough, and, moreover, if δ is small enough compared to the jitter and if the sequence of undelayed events before each introduced δ is long enough.

Both of the discussed cases are extremely rare, since the probability of event arrivals according to the nominal event arrival function with maximum positive or negative jitter is infinitesimal, whereas the typical jitter does not have a significant impact on the proposed analysis.

VI. EVALUATION

To study the impact of the attack parameters of a TDA on the response time of an observation task, we first explain how to model a PTP-based network for compositional performance

[10]Note that the scenario is unrealistically dramatized in Fig. 7 to allow for a more readable illustration.

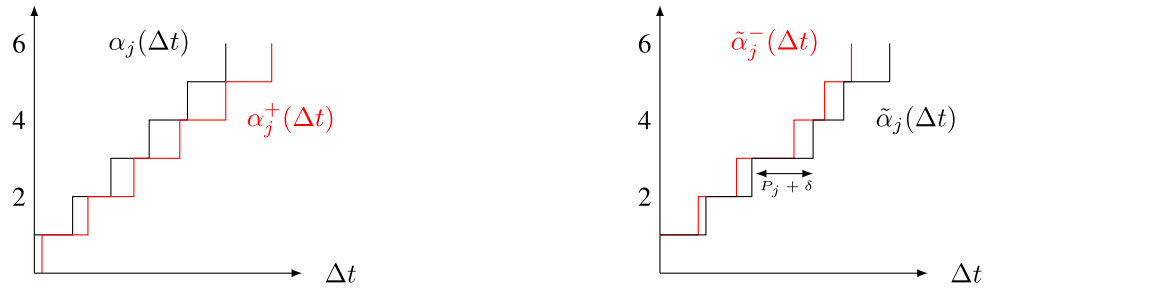

(a) Nominal event arrival function with maximum positive jitter compared to the nominal event-arrival function with zero jitter.

(b) Off-nominal event arrival function with maximum negative jitter compared to the off-nominal event arrival function with zero jitter.

FIGURE 7. Illustration of the impact of jitters on the event arrival function of a task τ_j.

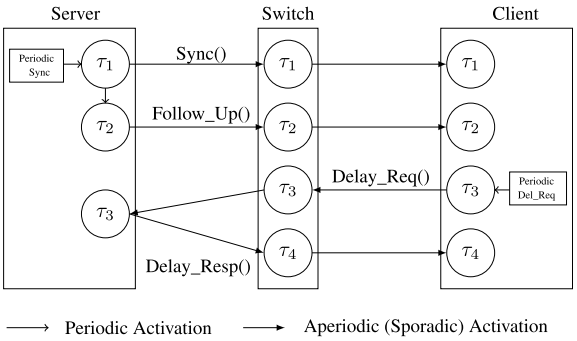

FIGURE 8. A simplified pyCPA model of an exemplary PTP-based system.

analysis (CPA), before we perform two experiments using pyCPA [21], namely, one based on synthetic task sets in Sec. VI-B and one based on an exemplary network with in Sec. VI-C.

A. MODELING FOR CPA

Fig. 8 illustrates a simplified compositional performance analysis (CPA) model of a PTP-based network, including a server node, a client node, and a PTP-aware switch. The output ports of the switch are mapped to CPA resources using a fixed-priority non-preemptive scheduling policy. On the switch, four tasks are depicted, which are required for performing the PTP synchronization operations (cf. Sec. II). For each task, it holds that the lower the index, the higher the priority. Note that in non-real-time operating systems such as Linux, PTP is implemented using one task only (the so-called PTP daemon). The decision to model PTP using four (sub-)tasks aims at modeling the effect of a TDA in a more fine-grained way.

The PTP message flow starts in the event source *Periodic Sync* on the server, which generates the periodic activation of *Sync*() messages, represented by task τ_1 in the server node. *Sync()* messages are propagated through the path, including task τ_1 in the switch, until the input port of the client node, where it activates task τ_1 on the client node. Task τ_2 represents the *Follow_Up()* message sent by the master node. The IEEE 1588-2019 standard requires that *Follow_Up()* is transmitted as early as possible after the transmission of the related *Sync()* message [4]. This message is propagated through the model in the same way as described for *Sync*(). In multi-cast communication, the IEEE 1588-2019 standard requires that the *Del_Req()* message is generated with a particular periodicity. Therefore, the event source (*Periodic Sync*) on the client node is used to activate task τ_3, which sends the message *Del_Req()* that is propagated through the switch until the input port of the server node. There, it activates the task τ_3, which creates the *Del_Resp()* message to be propagated until task τ_4 in the client node.

In the remainder of this work, we assume PTP to be modeled similarly in pyCPA, making adjustments as required for the respective experiment setups.

B. SYNTHETIC EVALUATION

In our first experiment, we explore the impact of different values of the attack parameters of a TDA on the WCRT of the observation task, applying our proposed analysis to synthetically generated task sets. To this end, we first introduce our experiment setup in Sec. VI-B1, before we discuss the results in Sec. VI-B2.

1) EXPERIMENT SETUP

In the course of this experiment, we generate sets of periodic tasks with cardinality 2 and 4, which share a resource under a fixed-priority preemptive scheduling policy. The utilization values of the tasks are generated using the UUniFast [22] algorithm such that a resource utilization of 80% is obtained, while their period P_i is chosen according to a uniform distribution over the interval $[5, 2500]$. For each task τ_i, the deadline is created according to a uniform distribution over the interval $[P_i, 10 \cdot P_i]$.

When simulating a TDA, the highest-priority task τ_j is assumed to be delayed by an amount of time δ, while the observation task τ_k is scheduled under the lowest priority. To carry out the analysis of each task set, pyCPA [21] was used.

2) RESULTS

The impact of different combinations of the attack parameters δ and ℓ_j of a TDA delaying a task τ_j on the response time of the

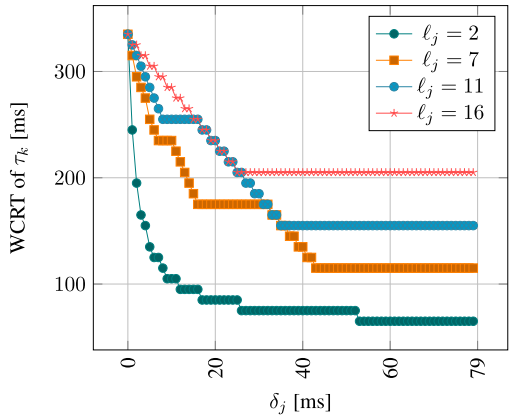

FIGURE 9. The impact of different values of the attack parameters δ and ℓ_j on the response time of the observation task τ_k.

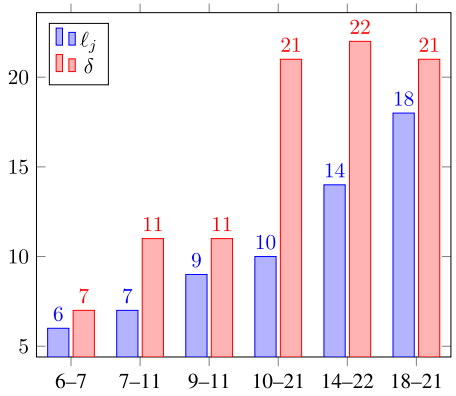

FIGURE 10. Different combinations of values of the attack parameters δ and ℓ_j leading to a busy window $w_k^{tda} = 255$ of the observation task τ_k.

observation task τ_k is portrayed in Fig. 9. It can be observed that with increasing length of the delay δ, the response time of τ_k decreases. Moreover, it is evident that the lower the value of ℓ_j, i.e., the more frequently a delay is introduced, the lower the response time of τ_k. However, the relations between δ and the response time of τ_k as well as between ℓ_j and the response time of τ_k are clearly not linear, but follow the dynamics elucidated in our analysis in Sec. V.

In Fig. 10, different combinations of values of the parameters δ and ℓ_j are presented, which all result in a busy window $w_k^{tda} = 255$ of the observation task τ_k. Following from this, it is evident that based on one observed response-time value of τ_k, it is not always possible to make a statement about the particular attack parameters of a TDA. Instead, it is more reasonable to enumerate and consider all possible attack scenarios.

C. USECASE EVALUATION

In our second experiment, we consider an exemplary usecase. The experiment setup is explained subsequently in Sec. VI-C1, before we discuss the results in Sec. VI-C2.

1) EXPERIMENT SETUP

As an exemplary usecase, we consider the distributed control and clock-sync network depicted in Fig. 11, as used, e.g., for

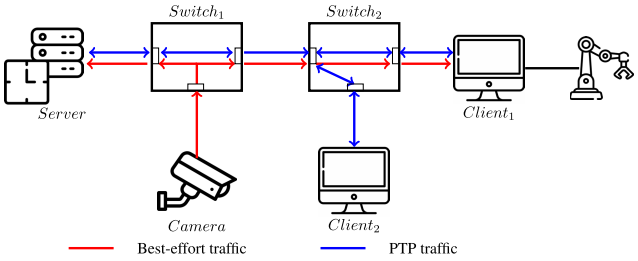

FIGURE 11. An industrial distributed control network considered as the usecase of our simulation.

TABLE 2. Packet sizes and time required for transmitting the packets, here considered as WCET.

Message/Packet	Packet Size (Byte)	WCET (μs)
Sync	106	9
Follow_Up	106	9
Delay_Req	106	9
Delay_Resp	116	10
Best Effort Traffic (Video)	875 - 1400	112

TABLE 3. Tasks considered in the experimental evaluation.

Task	Period
Sync (τ_j)	61 (P_Sync)
Delay_Req	61
Observation task (τ_k)	73.2 ($1.2 \times P\_Sync$)

robotic control, where typically update-rates in the order of microseconds are required. The network consists of a server and two clients, one of which is in charge of controlling a robot arm, and two PTP-capable switches. Moreover, the network comprises a video camera introducing mixed traffic.

When modeling the considered system, we follow a similar approach as proposed by Diemer *et al.* [21]: The system is modeled as an Ethernet AVB network, in which each client has input and output ports and each switch executes channel-delay tasks representing the default propagation and processing delays. Ports are modeled using a fixed-priority preemptive scheduling policy. Moreover, each output port accounts for the most significant arbitration delays. Static delays such as those caused by propagation in the communication channel are incorporated as constant-delay overhead in the paths. The analysis is performed using pyCPA [21].

Since the considered system is assumed to use an Ethernet 100BASE-TX network (100 Mbps), for each PTP synchronization message transmitted on the network, the payload is assumed to comply with the respective number of bits indicated by the IEEE 1588 standard [4], excluding additional bytes, i.e., the Ethernet header, the MACsec header, and the octets annexed at the physical link.[11] The size of each video packet is assumed to range from 875 bytes to 1400 bytes.

Table 2 summarizes the total length of the PTP and video packets as well as the respective WCET, i.e., here, the time

[11] For more information, refer to IEEE 802.3-2018 [23], Section 1.

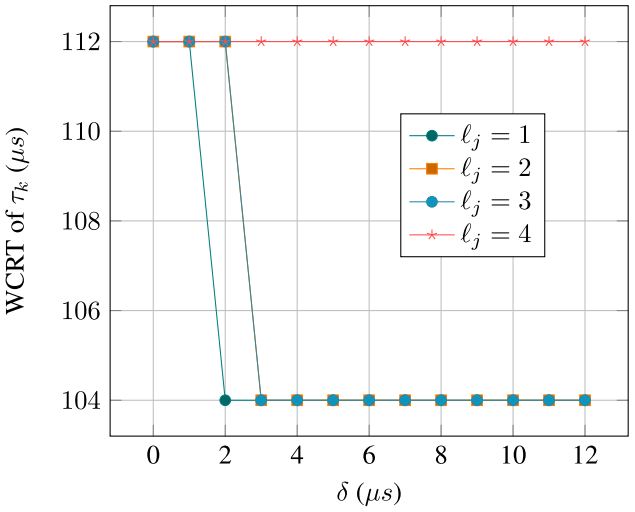

FIGURE 12. Impact of the attack parameters δ and ℓ_j on the response time of the observation task τ_k in the usecase simulation.

required for transmitting the packets at 100 Mbps. The timing characteristics of the PTP-related and observation tasks running on the client are given in Table 3.

2) RESULTS

In Fig. 12, the impact of the attack parameters δ and ℓ_j of a delayed task τ_j is depicted for different values of ℓ_j with δ being varied in discrete steps within the interval $[0, 12]\mu s$. It can be seen that the response time of the observation task τ_k is reduced from 112 μs to 104 μs for $\ell_j = 1$, $\ell_j = 2$, and $\ell_j = 3$ as soon as $\delta \geq 2\mu s$ ($\delta \geq 3\mu s$, respectively). However, no change is detectable for the same value of δ if $\ell_j = 4$. Concretely, this means, that a less frequently introduced delay has no impact in this case, whereas a more frequently introduced delay of the same length does. A corresponding behavior has already been observed in Fig. 9 in Sec. VI-B2, where, e.g., for $\ell_j = 2$ at time 20 the response time of the observation task τ_k is much lower than for $\ell_j = 16$.

Moreover, Fig. 12 gives the hint that the choice of the worst-case execution time of the observation task τ_k should be made very carefully. Depending on the task parameters of a specific usecase, the level of detail retrievable by means of the response time of the observation task can differ largely based on the considered parameters of the response time. Therefore, more fine-grained observations may be made by using different types of observation tasks. Exploring this, however, is beyond the scope of this work.

VII. CONCLUSION

Aiming to contribute to the development of more reliable and sensitive intrusion detection systems for PTP-based networks, we proposed to introduce observation tasks scheduled under the lowest priority on each client system. We showed, how, based on analysis techniques from the real-time domain, conclusions from the response time of an observation tasks to the existence of a TDA in the network can be drawn. Moreover, we analytically derived convergence properties of the busy window worst-case response time analysis methods, which do not only provide new theoretical insights, but can also be exploited to approximate attack parameters of an ongoing TDA.

De facto, the attack parameters derived in our analysis can serve as an additional input for sophisticated intrusion detection systems such as, e.g., the so-called Red-Zone Principle [18], allowing them to select better bounds for distinguishing off-nominal from nominal system behavior; thus, also enabling them to detect TDAs more reliably and to invoke mitigation strategies effectively. Optimizing such bounds for a specific intrusion detection system and determining the resulting false positive and false negative rates remains future work.

By means of comprehensive simulations, we explored the impact of different configurations of the attack parameters on the response time of an observation task and showed that different configurations can lead to the same response time of an observation task, emphasizing the importance of approximations, since the exact attack parameters cannot always be retrieved. Moreover, we discovered in our usecase simulation that the choice of the execution time of observation tasks is extremely important and has a strong impact on the detection sensitivity of an intrusion detection system.

REFERENCES

[1] T. Mizrahi, "A game theoretic analysis of delay attacks against time synchronization protocols," in *Proc. IEEE Int. Symp. Precis. Clock Synchronization Meas., Control Commun.*, Sep. 2012, pp. 1–6.

[2] M. Ullmann and M. Vögeler, "Delay attacks—Implication on NTP and PTP time synchronization," in *Proc. Int. Symp. Precis. Clock Synchronization Meas., Control Commun.*, Oct. 2009, pp. 1–6.

[3] E. Itkin and A. Wool, "A security analysis and revised security extension for the precision time protocol," *IEEE Trans. Depend. Sec. Comput.*, vol. 17, no. 1, pp. 22–34, Jan. 2020.

[4] *IEEE Standard for a Precision Clock Synchronization Protocol for Networked Measurement and Control Systems*, Standard 1588-2019 (Revision of IEEE Std 1588-2008), 2020, pp. 1–499.

[5] R. Annessi, J. Fabini, F. Iglesias, and T. Zseby, "Encryption is futile: Delay attacks on high-precision clock synchronization," 2018, *arXiv:1811.08569*.

[6] T. Mizrahi, *Security Requirements of Time Protocols in Packet Switched Networks*, document RFC 7384, 2014.

[7] W. Alghamdi and M. Schukat, "Precision time protocol attack strategies and their resistance to existing security extensions," *Cybersecurity*, vol. 4, no. 1, pp. 1–17, Dec. 2021.

[8] J. Tsang and K. Beznosov, "A security analysis of the precise time protocol (short paper)," in *Information and Communications Security*. Berlin, Germany: Springer, 2006, pp. 50–59.

[9] *IEEE Standard for a Precision Clock Synchronization Protocol for Networked Measurement and Control Systems*, Standard 1588-2008, Institute of Electrical and Electronics Engineers, 2008.

[10] *IEEE Standard for Local and metropolitan area networks-Media Access Control (MAC) Security*, Standard 802.1AE-2018 (Revision of IEEE Std 802.1AE-2006), 2018.

[11] S. Kent and R. Atkinson, *Security Architecture for the Internet Protocol*, document RFC 2401, Nov. 1998.

[12] G. Gaderer, A. Treytl, and T. Sauter, "Security aspects for IEEE 1588 based clock synchronization protocols," in *Proc. IEEE Int. Workshop Factory Commun. Syst.*, Jun. 2006, pp. 247–250.

[13] M. Han and P. Crossley, "Vulnerability of IEEE 1588 under time synchronization attacks," in *Proc. IEEE Power Energy Soc. Gen. Meeting (PESGM)*, Aug. 2019, pp. 1–5.

[14] B. Moussa, C. Robillard, A. Zugenmaier, M. Kassouf, M. Debbabi, and C. Assi, "Securing the precision time protocol (PTP) against fake timestamps," *IEEE Commun. Lett.*, vol. 23, no. 2, pp. 278–281, Feb. 2019.
[15] E. Lisova, M. Gutiérrez, W. Steiner, E. Uhlemann, J. Åkerberg, R. Dobrin, and M. Björkman, "Protecting clock synchronization: Adversary detection through network monitoring," *J. Electr. Comput. Eng.*, vol. 2016, pp. 1–13, Apr. 2016.
[16] C. Zimmer, B. Bhat, F. Mueller, and S. Mohan, "Time-based intrusion detection in cyber-physical systems," in *Proc. 1st ACM/IEEE Int. Conf. Cyber-Physical Syst. (ICCPS)*, Apr. 2010, pp. 109–118.
[17] N. Bellec, S. Rokicki, and I. Puaut, "Attack detection through monitoring of timing deviations in embedded real-time systems," in *Proc. ECRTS 32nd Euromicro Conf. Real-Time Syst.*, Modena, Italy, Jul. 2020, pp. 1–22. [Online]. Available: https://hal.inria.fr/hal-02559549
[18] M. Hamad, Z. A. H. Hammadeh, S. Saidi, V. Prevelakis, and R. Ernst, "Prediction of abnormal temporal behavior in real-time systems," in *Proc. 33rd Annu. ACM Symp. Appl. Comput.*, Apr. 2018, pp. 359–367.
[19] M. Hasan, S. Mohan, R. Pellizzoni, and R. B. Bobba, "Contego: An adaptive framework for integrating security tasks in real-time systems," in *Proc. 29th Euromicro Conf. Real-Time Syst. (ECRTS)*, vol. 76, M. Bertogna, Ed. Dagstuhl, Germany: Schloss Dagstuhl–Leibniz-Zentrum fuer Informatik, 2017, pp. 23:1–23:22.
[20] J. P. Lehoczky, "Fixed priority scheduling of periodic task sets with arbitrary deadlines," in *Proc. RTSS IEEE Comput. Soc.*, Dec. 1990, pp. 201–209.
[21] J. Diemer, J. Rox, and R. Ernst, "Compositional performance analysis in Python with pyCPA," in *Proc. WATERS*, 2012, p. 46. [Online]. Available: http://retis.sssup.it/waters2012/accepted/102_Final_paper.pdf
[22] E. Bini and G. C. Buttazzo, "Measuring the performance of schedulability tests," *Real-Time Syst.*, vol. 30, nos. 1–2, pp. 129–154, May 2005, doi: 10.1007/s11241-005-0507-9.
[23] *IEEE Standard for Ethernet*, Standard 802.3-2018 (Revision of IEEE Std 802.3-2015), 2018, pp. 1–5600.

LEA SCHÖNBERGER (Graduate Student Member, IEEE) received the B.Sc. degree in computer science from the University of Münster, Germany, in 2014, and the M.Sc. degree in computer science from TU Dortmund University, Germany, in 2017, where she is currently pursuing the Ph.D. degree in computer science. Since September 2017, she is a Research Associate at TU Dortmund University, where she was a member of the Design Automation for Embedded Systems Group, Department of Computer Science, before she switched to a half-time position in the Databases and Information Systems Group, Department of Computer Science, along with a half-time position in the AG Embedded Systems, Department of Electrical Engineering and Information Technology, in August 2020. Her research interest includes embedded and distributed systems and focuses particularly on end-to-end quality of service guarantees and autonomous systems. She was a member of the Artifact Evaluation Committee of the IEEE Real-Time Systems Symposium (RTSS) 2020 and served as a Reviewer for the IEEE TRANSACTIONS ON COMPUTER AIDED DESIGN OF INTEGRATED CIRCUITS and SYSTEMS (TCAD).

MOHAMMAD HAMAD received the B.Eng. degree in software engineering and information system from Aleppo University, Syria, in 2009, and the Ph.D. (Dr.-Ing.) degree in computer engineering from the Institute for Data Technology and Communication Networks, Technical University of Braunschweig, Germany, in 2020.

Since 2020, he has been a Postdoctoral Researcher with the Embedded Systems and Internet of Things Group, Faculty of Electrical Engineering and Information Technology, Technical University of Munich (TUM). His research interests include autonomous vehicle and the IoT security.

JAVIER VELASQUEZ GOMEZ received the B.S. degree in electronic engineering from the National University of Colombia, in 2005, the M.S. degree in business administration in technology management from the Northern Institute of Technology, Hamburg, in 2019, and the M.Sc. degree in information and communication system from the Hamburg University of Technology, Germany, in 2020.

Since 2020, he has been working with NXP Semiconductors, where he is managing innovation projects in the field of TSN and wireless communication, especially 5G mobile networks for industrial applications.

SEBASTIAN STEINHORST (Senior Member, IEEE) received the M.Sc. (Dipl.-Inf.) and Ph.D. (Dr.Phil.Nat.) degrees in computer science from Goethe University, Frankfurt, Germany, in 2005 and 2011, respectively.

He is currently an Associate Professor at the Technical University of Munich (TUM), Germany. He also leads the Embedded Systems and Internet of Things Group, Department of Electrical and Computer Engineering. He was also a Co-Program PI with the Electrification Suite and Test Laboratory, Research Center TUM-CREATE, Singapore. His research interests include design methodology and hardware/software architecture co-design of secure distributed embedded systems for use in the IoT, automotive, and smart energy applications.

SELMA SAIDI (Member, IEEE) received the Ph.D. degree in computer sciences from the University of Grenoble, France, in 2013, conducted together with STMicroelectronics.

After her Ph.D., she joined the Technical University of Braunschweig, as a Postdoctoral Researcher, and later the Hamburg University of Technology, as a Permanent Research Scientist. Since 2020, she has been a Professor of embedded systems with TU Dortmund University. Her key aspects are the development of novel hardware and software design methods for embedded and autonomous systems where performance, predictability and self-adaptability play an important role. Her domains of applications are avionics, autonomous driving, and the Internet of Things. Her research interests include the design, implementation, and validation of innovative intelligent embedded systems. She participates regularly as a TPC member in leading conferences in embedded systems design and real-time systems, such as DAC, DATE, and RTSS.